Results from a Prototype MAPS Sensor Telescope and Readout System with Zero Suppression for the Heavy Flavor Tracker at STAR

L. Greiner[1,4], H.S. Matis[1], H. G. Ritter[1], A. Rose[1], T. Stezelberger[1], X. Sun[2], M. Szelezniak[3], J. Thomas[1], C. Vu[1], H. Wieman[1]

1 Lawrence Berkeley National Laboratory, Berkeley, CA 94720
2 Institute of High Energy Physics, Beijing 100039, China
3 Institut Pluridisciplinaire Hubert Curien, Strasbourg, France

4. Contact Author – Full contact information –
Leo Greiner
Lawrence Berkeley National Laboratory
MS 70R0319
Berkeley, CA 94720
(voice) 510-486-7274
(fax) 510-486-4818
LCGreiner@lbl.gov

ABSTRACT

We describe a three Mimostar-2 Monolithic Active Pixel Sensor (MAPS) sensor telescope prototype with an accompanying readout system incorporating on-the-fly data sparsification. The system has been characterized and we report on the measured performance of the sensor telescope and readout system in beam tests conducted both at the Advanced Light Source (ALS) at Lawrence Berkeley National Laboratory (LBNL) and in the STAR experiment at the Relativistic Heavy Ion Collider (RHIC). This effort is part of the development and prototyping work that will lead to a vertex detector for the STAR experiment.

Keywords: APS, Pixel, Vertex detector, MAPS, STAR

INTRODUCTION

We are conducting research and development with the goal of constructing a vertex detector for the STAR experiment at RHIC [1]. The primary physics requirement for this detector upgrade is to provide vertex pointing capability to resolve vertices of D^0 and other heavy flavor decays displaced from the primary interaction vertex by about 100-150 μm [2]. This requirement leads to design goals for the vertex tracking detector that include a radiation length of < 0.5% / layer and pixel positional stability to 20 μm. In this stringent environment, the mechanical design requirements interact strongly with the sensor and readout electronics design. Sensors thinned to 50 μm, air cooling and aluminum conductor readout cables become necessary constituents of the candidate design. The expected final system design is an array of 33 sensor ladders with ten 2 cm × 2 cm sensors / ladder and parallel independent ladder readout systems. We intend to operate the system at the ambient temperature in the STAR experimental area (approximately 25° C). We are pursuing an incremental approach to reaching the final arrangement by designing and constructing prototype generations of sensors and readout electronics. Using first generation Mimostar2 MAPS prototypes [3], we have constructed a three sensor array in a telescope configuration and a prototype readout system that includes on-the-fly data sparsification. We report on the performance of this prototype system in a test beam of 1.2 GeV electrons at the ALS at LBNL and in the STAR detector at RHIC during the 2006-2007 200 $\sqrt{s_{NN}}$ GeV Au - Au run.

SYSTEM DESIGN

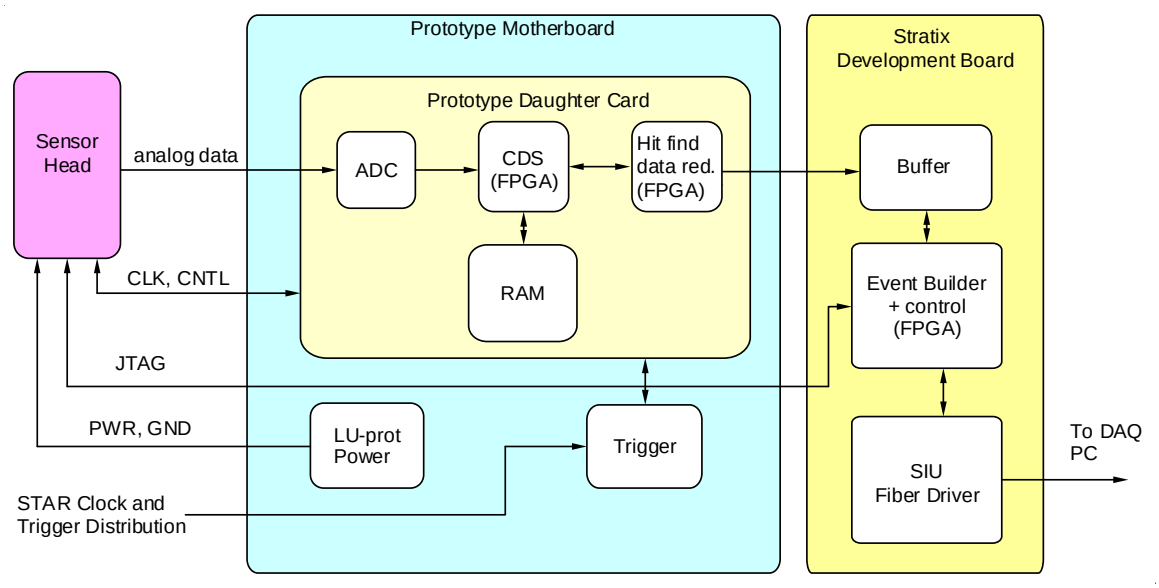

Figure 1: A schematic representation of the readout system.

The prototype system is composed of four functional blocks as presented in figure 1. The sensor head contains the three Mimostar2 sensors and the associated discrete component buffers/drivers. This head assembly is connected via individually shielded CAT-5 twisted pair cables to a motherboard, where the analog signals are routed to a daughter card to be digitized and processed. The daughter card performs correlated double sampling (CDS) and data reduction through a real time cluster finding algorithm. The cluster address data is buffered, built into an event, and transferred to our data acquisition PC using a commercial Altera Stratix field programmable gate array (FPGA) development board (SDB) and a fiber optic connection. Latch-up protected power, clocks, resets and Joint Test Action Group (JTAG) communication are provided to the sensor head from the motherboard/SDB combination. External triggers are accepted into the motherboard/daughter card. The system is run continuously and data flows through the digitization, CDS and cluster finding synchronously with a 50 MHz clock. A fiber optic cable transmits the events, which are accumulated and built in response to a trigger, into the data acquisition PC (DAQ).

DEPLOYED HARDWARE

We are using Mimostar2 sensor prototypes which are a type of Monolithic Active Pixel Sensors developed by IPHC in Strasbourg, France. These sensors contain a 128 × 128 array of 30 μm pixels and are fabricated in the 0.35 μm Austria Micro Systems CMOS process. The Mimostar2 has a well developed interface and control system with multiple synchronization input and output pads and configuration via an industry standard JTAG interface. This interface provides control of internal configuration registers that select such parameters as internal gain, output type (single ended or differential), bias settings and internal column masking.. We are using the single multiplexed analog differential current output with a readout clock of 50 MHz. This sensor is designed to mimic the readout of a much larger sensor by adding dummy pixels to give an apparent size of 640 × 128. The dummy data is discarded in our analysis, but lengthens the sensor integration time to 1.7 ms. The Mimostar2 sensor is a development prototype and contains two separate types of pixel design in two 64 × 128 arrays. The first array is the standard IPHC pixel, whilst the second is a radiation hardened design [4].

The full die thickness sensors are mounted to 2 layer 25 μm Kapton flex cables which are glued to aluminum frames that hold the sensors with a planar spacing of 2.7 mm. A photograph of the telescope head assembly is shown in figure 2. The daughter card is a small card edge printed circuit board containing a Xilinx XC2V100 Virtex2 FPGA, TI ADS5270 8-channel, 12-bit ADC and two 18Mb GSI GS8162Z72C SRAM chips. This is the heart of the readout and data reduction system where triggers are processed, analog signals digitized, CDS and cluster finding performed, and cluster addresses buffered. The motherboard supplies the latch-up protected regulated power to the sensors, accepts external triggers, configuration and control, and provides the interconnection between the sensor head, the daughter card and the SDB. The SDB features PMC connectors for attachment of our fiber optic readout board, an Altera Stratix FPGA, a bus structure for communication with the daughter card, and a well developed set of configuration and I/O ports. The FPGA provides the control logic for

event building, fiber optic transfer module control and sensor head JTAG configuration. We use the Source Interface Unit (SIU) and Readout Receiver Cards (RORC) [5] developed for use at the ALICE experiment at CERN as our optical link hardware to transfer data to and from the STAR DAQ system.

Figure 2: Picture of three sensor Mimostar2 telescope mounted in the plastic housing head.

The basic data flow during normal data taking is as follows. Analog differential current signals from the Mimostar2 sensors are converted to voltage mode and conducted out of the telescope head assembly over shielded twisted pair cables with a 50 MHz sample clock. The signals are digitized in a 12 bit ADC and the data passed synchronously with the read clock into SRAM. The SRAM is configured as an updating array of ADC values corresponding to the pixels of the sensor. It stores one sensor frame of ADC data. We perform CDS for each pixel synchronously with the 50 MHz sample clock cycle. The ADC value of the current pixel is subtracted from that pixel's value in the previous frame in order to evaluate the charge deposited in the pixel during the past integration time and to remove fixed pattern noise. The current pixel ADC value is written into the SRAM and the result of the subtraction is passed to the next stage for data reduction through cluster finding. The multiplexed serial data output stream from the sensor is resorted in order to reconstruct the geometry of the pixel array and to perform a raster scan through the array. This allows for the identification of clusters by doing threshold pattern recognition. This procedure is performed in the daughter card FPGA over a synchronous window that examines a sequential 3×3 array of pixels. A diagram describing the implementation of this algorithm is shown in figure 3.

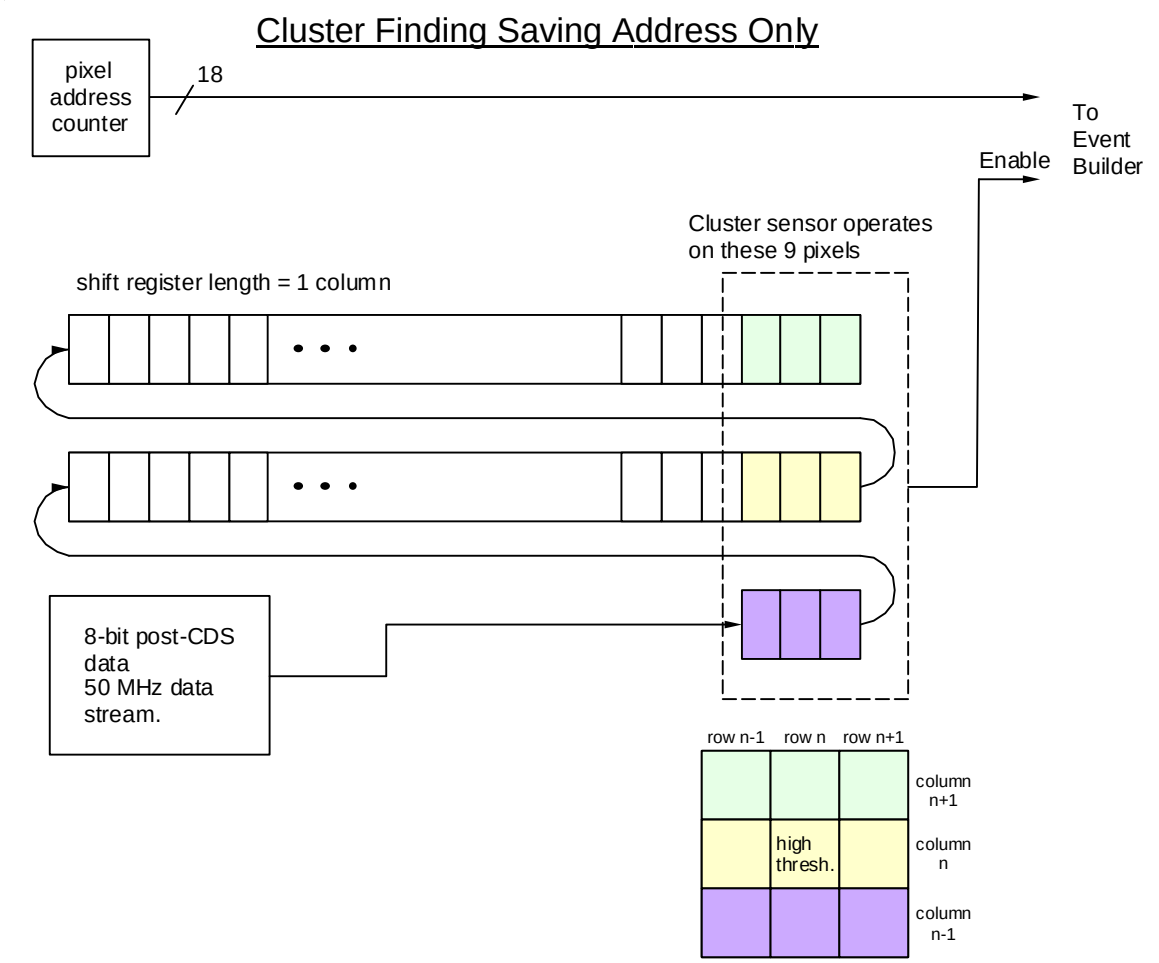

Figure 3: Schematic representation of a simple cluster finding algorithm for the vertex detector. Post CDS ADC data from two Mimostar2 detector columns + 3 pixels are fed sequentially in an 8-bit wide shift register. The center pixel ADC value of a 3 × 3 pixel window is compared to a threshold with each clock tick. If the center pixel threshold is exceeded, additional cluster identification criteria are checked for the 3 × 3 pixel window. If the results meet the critera for a cluster, the center pixel address is stored into a readout FIFO. This method is extendable to allow for multiple simultaneous thresholds and geometric pattern triggers.

When the threshold criteria are met, typically by a center pixel exceeding a threshold value with at least one of the eight surrounding pixels exceeding a lower threshold value, the 18-bit address of the center pixel is presented to an event FIFO. This event FIFO is enabled for one frame of data when a trigger is received from the STAR trigger system. The cluster address data are then bundled with the received trigger event ID, built into our event structure, and transferred to the STAR DAQ receiver PC over a high-speed bi-directional fiber link. The raw data rate from our ADCs of the telescope head is 225 MB/s. With an average occupancy of 20 hits/sensor per frame and an 1 kHz readout, the data rate is reduced (with event structure overhead) to about 612 kB/s. The efficiency of this data sparsification system will translate directly to the larger systems that we will develop for the final detector. In addition to the normal sparsified data taking mode, this

system can also be configured with an FPGA firmware change to readout continuous frames of ADC values from a single sensor at a time. Bandwidth limitations prevent us from reading out more than a single sensor in this full frame mode of data acquisition.

PERFORMANCE

The assembled system was calibrated with a ^{55}Fe source. The average noise observed for both pixel types was about 6.5 ADC counts. The ^{55}Fe calibration peak was measured at the level of 350 and 300 ADC counts for the standard and radiation tolerant diodes, respectively. These values translate to an electron noise charge (ENC) of about 30 and 35 electrons at the ambient temperature of about 28º C. Previous tests of the Mimostar2 chip completed at IPHC showed that the sensor is capable of reaching noise performance at the level of about 11-15 electrons at 30º C. The measured noise in the telescope system was dominated by the Mimostar2 sensors themselves. The unexpectedly high noise value was found to be related to the system structure. Mimostar2 was a small size prototype with many outputs intended only for testing purposes. When the telescope system was designed, the layout of the flex cables, to which the chips were to be mounted, was optimized for minimum size and minimum mass as would be expected in the final detector. This flex cable design left some chip output pads un-bonded and a set of un-terminated Mimostar2 internal DAC outputs were responsible for the measured increase in the noise level. Accommodating existing accelerator schedules did not allow time for a redesign and re-fabrication of the flex cables and consequently the measurements shown below are at a noise level higher than what the sensor is capable of in an optimized environment.

We measured the performance of this prototype system in a test beam of 1.2 GeV electrons at the Advanced Light Source (ALS) in the Booster test facility beamline. The ALS booster operates as a pulsed machine with a two second repetition rate. A trigger signal was provided by the ALS facility. We used the continuous full frame mode of data acquisition, where we read raw ADCs for multiple frames from a single sensor, to test sensor performance for minimum ionizing electrons. In the enclosed sensor head, the noise performance degraded moderately to about 34 and 38 electrons for the standard and radiation tolerant structure, respectively. This change is likely due to an increased operating temperature. The temperature of the sensors enclosed in the head was not measured and we estimate it to be 5-10 degrees hotter than ambient.

In the full-frame readout mode, a Landau distribution for minimum ionizing particles was clearly observed. Plots showing the distribution of signal in seed pixels are presented in figure 4.

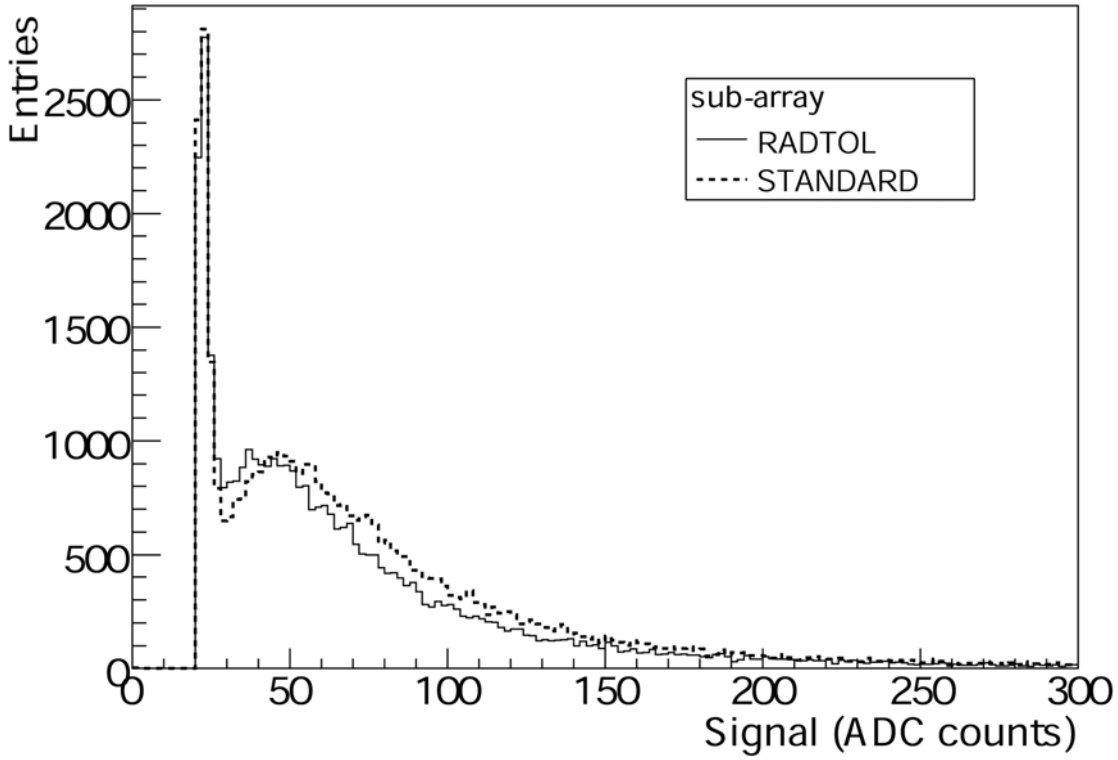

Figure 4: Landau shaped data collected with one plane of the telescope prototype in the full-frame readout mode.

The observed most probable value (MPV) is at 49 and 43 ADC counts for standard and radiation tolerant structure, respectively which corresponds to approximately 230 electrons.

A set of runs with different cuts on the central and neighboring pixel in the cluster finder was taken in the normal readout mode. The cut on neighboring pixels was set to 14 ADC counts (approximately 2 × noise value) and the cut on the central pixel varied from 20 to 150 ADC counts. In order to simultaneously achieve high efficiency and low accidentals, we used relatively low cluster finder threshold settings. These settings yielded typically 2-3 pixel addresses per track point. These adjacent cluster addresses were merged in the data analysis and assigned to a single location. To estimate the efficiency of each layer separately the other two layers are used as reference planes on a frame by frame basis. If a hit in one of the reference planes has a companion in the other plane, at the same location and within a specified search window, then it is said they are associated with a track. The presence of a hit in the third layer within a specified search window indicates that the layer was efficient. At the same time, if there are hits in the layer of interest that are not part of tracks and cannot be associated with any hit in any other layer within the search window, the hits are classified as noise generated accidentals. In case the hit in the layer of interest is not a part of a track, and can be associated with one hit in any of the two other layers, it is assumed to be a part of the track and influences neither efficiency nor accidental counts. The plots of detection efficiency and accidental rate as functions of cut on the central pixel are presented in figure 5 and figure 6. As one can see, the efficiency and accidental rates of our system

suffer from the increased noise of the sensors. In optimum conditions, with a sensor ENC of 11-15 electrons, the algorithms are expected to have efficiency greater than 99% with less than a 10^{-4} accidental rate.

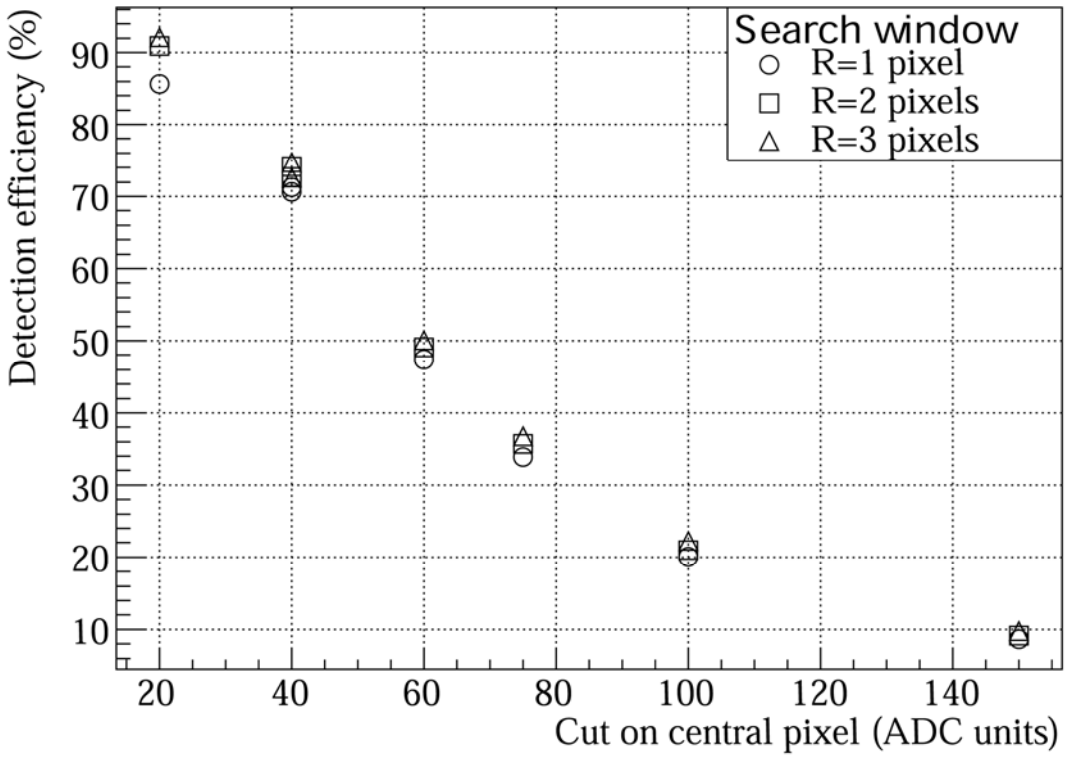

Figure 5: Detection efficiency of telescope layers as a function of the applied cuts and search window radius.

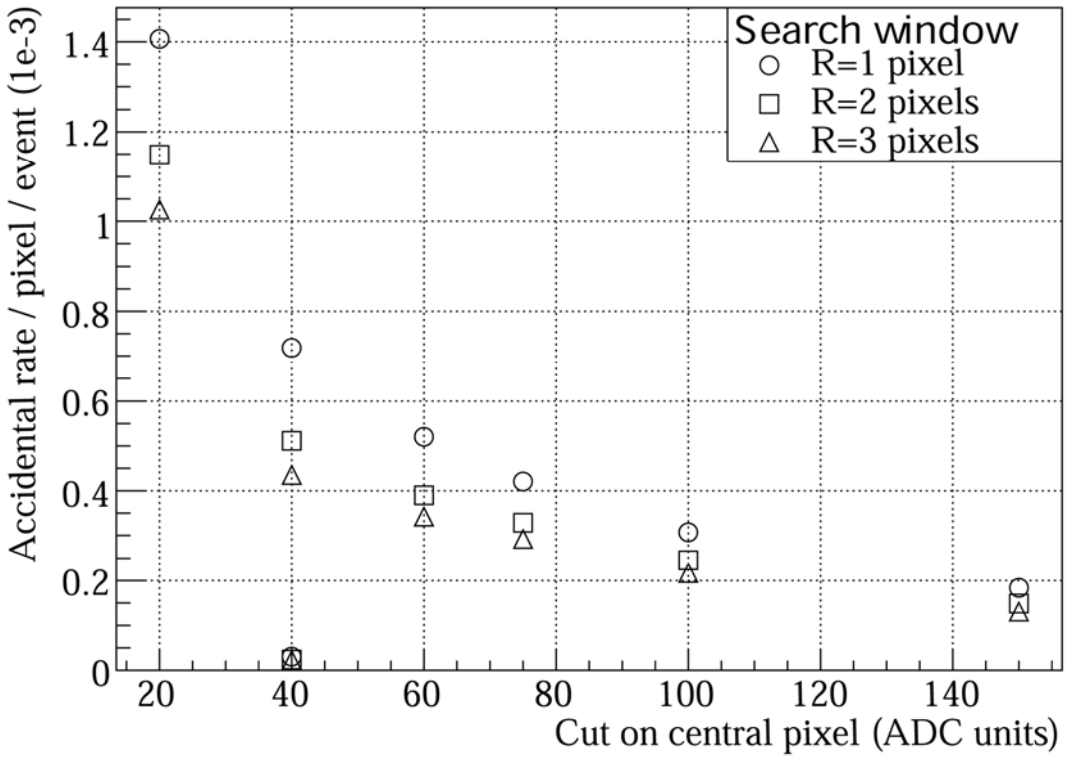

Figure 6: Accidentals rate per pixel and per frame for all three telescope layers as a function of the cuts applied and search window radius.

After the set of initial beam tests at the ALS, the system was moved to BNL for installation into the STAR detector for the last three weeks of the 2006-2007 Run 7 running period at RHIC. The sensor head was placed near the interaction diamond with the sensor plane approximately perpendicular to the beam axis at a final location of about 145 cm from the interaction region center along the beam axis and about 5 cm below the beam pipe. The electronics readout box containing the motherboard/daughter card/SDB assembly was located inside the STAR magnet pole tip at approximately the position expected to be used for the final detector electronics. The telescope operated in a uniform magnet field at 0.5 T, the nominal field for STAR.

It was the goal of this test to measure sensor and system performance in the STAR environment, to check for electronic and environmentally produced noise, to measure the charged particle density in STAR and to do limited tracking. In addition, the integration of a prototype readout system with the existing STAR trigger, data acquisition, and control subsystems constitutes an important system design milestone.

The measured noise in the system installed in STAR was 7.48 ADC counts, comparable to the laboratory and ALS environments. The noise level remaining comparable through our tests in the laboratory, at the ALS and in the STAR detector, validates our system and electronics designs. However, the overall increased noise level from the lack of sensor DAC termination could still mask some small environmentally induced noise increase. The charged particle density through our sensor telescope at STAR during normal running (with a 1.7 ms integration time) was about 3.9 merged clusters per sensor. The average luminosity during the time that our sensors were at

STAR was 8×10^{26} $cm^{-2}s^{-1}$. This charged particle density roughly agrees with our existing simulations and indicates that the chosen pixel technology is appropriate for use with the observed tracking environment.

During the STAR regular running period, we took data triggered via the standard STAR interface to the STAR trigger subsystem. Our integration time ensures that we will have 1.7 ms of STAR interactions read out in each sensor frame. Some of the integrated tracks are background, which can be expected to originate from beam-gas type interactions. The majority of tracks from this type of background should be roughly parallel to the beam axis. Tracks from interactions in the STAR vertex diamond should have a characteristic angular distribution in the beam axis plane. A plot of the angular distribution of tracks registered by our sensor telescope is shown in figure 7 (all with arbitrary scaling). One can see our measured peak in the angular distribution and the geometrically calculated peak based on the known distribution of tracks from the STAR interaction diamond. In this region, the angular value matches well but our measured distribution is wider. We are currently investigating this and conjecture that it could be due to scattering in the STAR beam pipe. For a part of the run, the beams at RHIC were displaced such that they did not collide at the STAR intersection region. The angular distribution of tracks corresponding to beam – gas interaction and other backgrounds is also shown for that period. The distribution is peaked at an angle of 0 degrees (parallel to the beam).

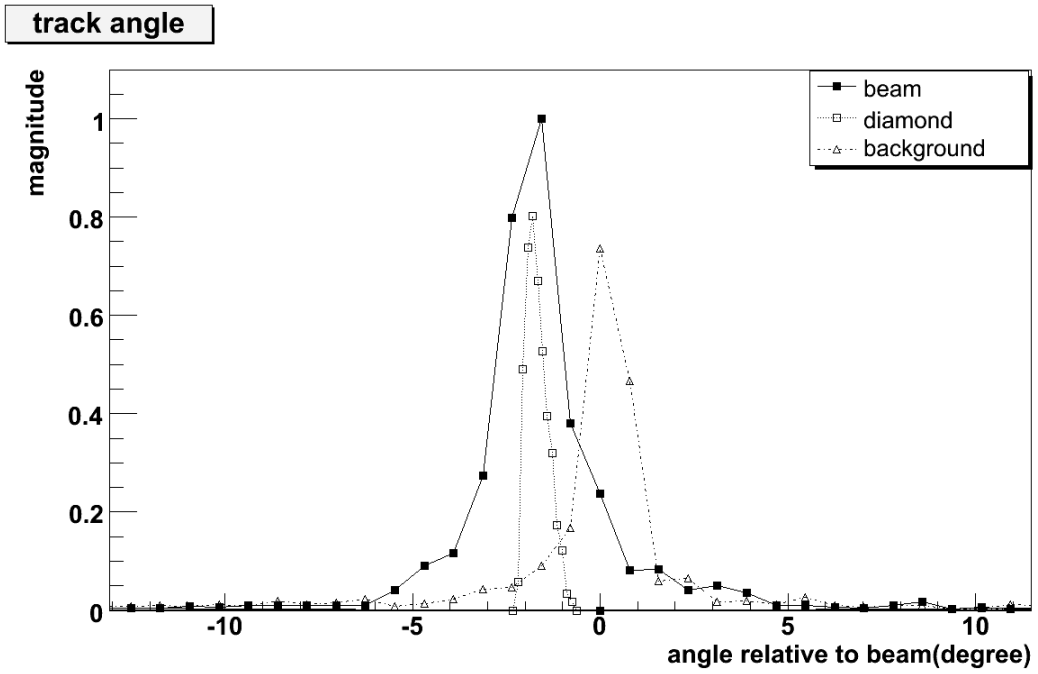

Figure 7: Angular distribution of tracks in the sensor head. The calculated distribution that corresponds to the interaction diamond at STAR is shown as well as the measured angular distribution when the sensor was triggered by the STAR trigger during normal beam interaction data taking. The background angular distribution was taken during special running mode where the RHIC beams were displaced such that there were no collisions in the interaction region and corresponds to beam – gas interactions and other backgrounds.

HOT PIXELS and RADIATION DOSE

A small number of MAPS pixels show a large variation in signal level from frame to frame and thus a large difference in the CDS measurement. We call these aberrant signals "hot pixels." Before the detector was inserted into the STAR magnet, we measured a total of 18 hot pixels. When we measured the last data set, we found at most an addition of 3 extra hot pixels.

We also measured the total radiation dose exposure of the telescope by putting a thermo-luminescent dosimeter (TLD) on the telescope head assembly housing. An analysis of the TLD that was located near the sensor head showed that it had a radiation dose of 325 rad integrated over the running time. This measurement will be used to help design sensors that meet the requirements of the final design.

SUMMARY

We present a preliminary system design and data taken with a prototype system as part of the effort for development of a vertex detector for use at STAR. This system is an early prototype whose performance is evaluated as part of the overall vertex detector development effort. We have successfully implemented a continuous readout 50 MHz data acquisition system with on-the-fly data sparsification that gives near three orders of magnitude data reduction from the raw ADC rates. This readout system has been mated with prototype Mimostar2 sensors and configured as a telescope system to measure the charged particle environment in the STAR environment near the final detector position. We find that the system works well, gives reasonable efficiency and accidental hit rates, and measures an angular distribution of tracks consistent with imaging the interaction diamond and with imaging beam-gas interaction type background. The prototype readout system integrated well into the existing STAR electronics and trigger infrastructure and functioned successfully as another STAR detector subsystem.

ACKNOWLEDGEMENTS

We gratefully acknowledge the assistance of David Malone and Warren Byrne at the ALS and of Bob Souza and Ken Asselta at the STAR hall at RHIC. We would also like to acknowledge Marc Winter and the IPHC group for the development of the Mimostar2 sensors. This work received support in part from the US Department of Energy – Contract no. DE-AC02-05CH11231, Office of Nuclear Physics.

References

[1] J. Adams, M.M. Aggarwal, Z. Ahammed, J. Amonett, B.D. Anderson, D. Arkhipkin, et al.
Experimental and theoretical challenges in the search for the quark-gluon plasma: The STAR Collaboration's critical assessment of the evidence from RHIC collisions,
Nuclear Physics A, Volume 757, Issues 1-2, First Three Years of Operation of RHIC, 8 August 2005, Pages 102-183.

[2] S. Kleinfelder, S. Li, F. Bieser, R. Gareus, L. Greiner, J. King, et al.
A proposed STAR microvertex detector using Active Pixel Sensors with some relevant studies on APS performance,
Nuclear Instruments and Methods in Physics Research Section A, Volume 565, Issue 1, Proceedings of the International Workshop on Semiconductor Pixel Detectors for Particles and Imaging - PIXEL 2005,
1 September 2006, Pages 132-138.

[3] Deptuch, G.; Berst, J.-D.; Claus, G.; Colledani, C.; Dulinski, W.; Gornushkin, Y.; et al. Design and testing of monolithic active pixel sensors for charged particle tracking
IEEE Transactions on Nuclear Science,
Volume 49, Issue 2, Part 2, April 2002 Page(s):601 - 610
doi:10.1109/TNS.2002.1003683

[4] Dulinski, W.; Besson, A.; Claus, G.; Colledani, C.; Deptuch, G.; Deveaux, M. ; et al. Optimization of tracking performance of CMOS monolithic active pixel sensors
IEEE Transactions on Nuclear Science,
Volume 54, Issue 1, Part 2, Feb. 2007, Page(s):284 - 289
doi:10.1109/TNS.2006.889167

[5] http://alice-proj-ddl.web.cern.ch/alice-proj-ddl/